

## Liquid Film Adhesion in Contact between Rough Surfaces

PhD. stud. Eng. Amir ROSTAMI<sup>1</sup>, Prof. PhD. Eng. Jeffrey L. STREATOR<sup>2</sup>

<sup>1</sup> Georgia Institute of Technology, amir.rostami@gatech.edu

<sup>2</sup> Georgia Institute of Technology, jeffrey.streator@me.gatech.edu

**Abstract:** Many micro and nano scale devices are influenced by the presence of liquid at the interface between contacting surfaces. Such liquid may induce large and undesired adhesive or “stiction” forces. In some cases, liquid may find its way into the interface of two rough surfaces that are already in contact. It is of interest to model the manner in which the interface proceeds to a new equilibrium configuration upon introduction of the liquid. Such a process involves interactions among viscosity, elasticity and capillarity. To simulate such effects, a contact model is employed to account for surface deformation, a mixed-lubrication model is applied to analyze liquid flow and the Young-Laplace equation is implemented at the boundary of the wetted region to provide the capillary pressure. Calculations are performed to reveal the roles of liquid viscosity, liquid surface tension, surface roughness and elastic modulus on the generation of adhesive forces.

**Keywords:** Capillary flow, Surface roughness, Liquid-mediated adhesion

### 1. Introduction

Many natural and engineered systems involve a thin liquid film between two solid surfaces. Familiar examples in nature include: plants and trees, which transport fluid from roots to leaves in opposition of gravity through xylem conduits [1]; and soils whose strength characteristics depend on the way water interacts between solid particles [2]. Among engineered systems, there are several small scale devices for which liquids are present in confined regions during fabrication or during operation [3, 4]. In many cases, the presence of the liquid film causes excessive adhesive forces and device failure [5, 6]. On the positive side, in the operation of nanofluidic devices, capillary forces operating in submicron channels are used to pump liquids from one location to another [7, 8]. In this work, a model for the capillary flow between two nominally flat rough surfaces is presented. The current model represents an extension to the previous published models of liquid-mediated adhesion. Streator and Jackson [9] and Streator [10] presented 2D spectral and deterministic approaches, respectively, to model liquid-mediated adhesion between rough surfaces. Rostami and Streator extended the 2D liquid-mediated adhesion models to 3D models using a spectral approach [11, 12] and a deterministic approach [13]. These former analyses are restricted to static conditions (i.e., do not consider flow) and treats the free surface of the liquid in only an average sense namely that the film thickness at the periphery of the film is equated with the global average spacing between the surfaces.

### 2. Methodology

A schematic plot of the interface of interest is shown in Fig. 1. The wetting liquid spreads between an annular rigid flat punch and a rough disk until its radius,  $b$ , reaches the outer radius of the punch,  $r_o$ . The liquid is introduced at the inner radius of the punch,  $r_i$ , and the capillary effect is the driving force for the liquid flow. The large concave curvature at the free surface of the liquid causes a pressure drop across the free surface, which drives the liquid between the two surfaces. The pressure at the inner radius of the punch is ambient, and at the outer boundary of the liquid film, the negative pressure can be obtained from Laplace-Young relation [14]. The negative pressure within the capillary film induces tensile stresses in the interface. The compressive stresses arising at solid-solid contact spots oppose the tensile stresses due to capillary effects.

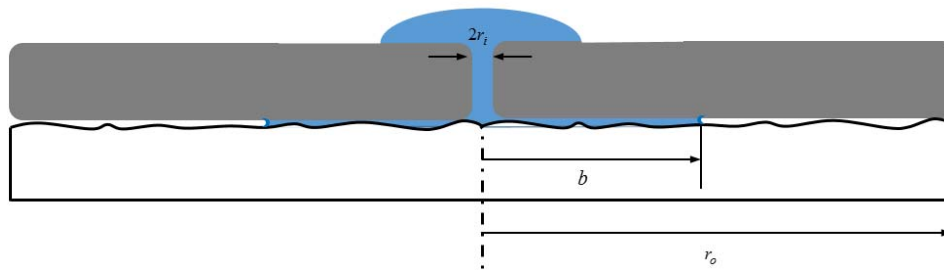


Fig. 1. Schematic depiction of the modeled interface.

In this work, a model is developed to study the capillary flow between the surfaces depicted in Fig. 1. The model is comprised of a macro-contact model, a micro-contact model and a mixed lubrication model. The macro-contact model is used to determine the pressure distribution within the nominal region due to external load acting on the contacting surfaces. In macro-contact model, the effect of surface roughness is neglected, so that the contacting surfaces are assumed to be smooth. The surface roughness effects are considered in the micro-contact model where the local gap is calculated. The hydrodynamic pressure distribution within the liquid flow due to the capillary effects is obtained from the mixed lubrication model. An iterative numerical algorithm is designed to solve the three sub-models simultaneously to obtain the results for the tensile force, liquid flow rate and local gap between the two contacting surfaces.

## 2.1 Macro-Contact Model

In the macro-contact model, the pressure distribution under a rigid annular punch deforming an elastic half-space is evaluated. A schematic view of this problem is shown in Fig 2. The pressure distribution and displacement field for the contact of an annular rigid punch and an elastic half space under external loading of  $P_{ext}$  can be obtained numerically via influence coefficients. The influence coefficients are derived from the analytical surface deformation solution of an elastic half-space under uniform pressure [15]. A finite radius of curvature is assumed for the edges of the rigid punch to avoid unbounded contact pressures. Results for the contact pressure distribution under a rigid punch with inner and outer radii of  $r_i = 1$  mm and  $r_o = 3$  cm respectively and with edge radius of  $r' = 0.1$  mm under the penetration of  $d = 0.1$   $\mu\text{m}$  is given in Fig. 3.

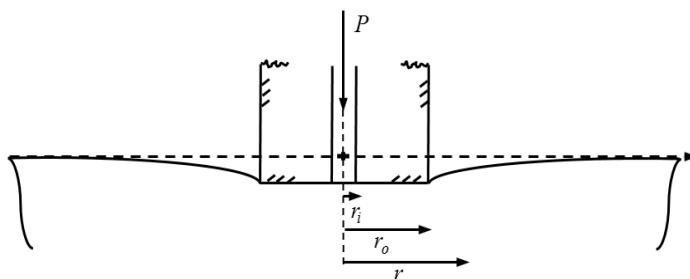


Fig. 2. Illustration of surface deformation in a half-space deformed by an annular rigid punch.

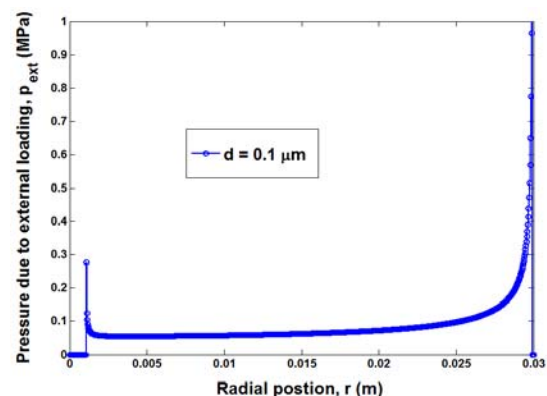


Fig. 3. Pressure distribution under the rigid annular punch.

## 2.2 Macro-Contact Model

On a micro-level, all surfaces have some degrees of waviness or roughness. The pressure distribution from the macro-contact model along with the hydrodynamic pressure within the liquid flow cause surface deformation in the contacting rough disk at micro levels. In the current model, the Jackson and Streater (JS) multiscale model is used to model the contact at micro-scale level. The JS model is based on representing the rough surface in multi scales of roughness using the fast Fourier transform (FFT) of the surface heights. The rough surface data is generated employing a surface profile generation method outlined by Garcia and Stoll [16]. A two dimensional FFT is then performed on the generated surface heights to obtain the amplitude at each frequency level as is performed in [17]. At each frequency level, the asperities are modelled assuming a three-dimensional sinusoidal geometry. The relation between average gap and the average pressure at frequency level is given by [18]

$$\frac{\bar{g}_k}{\Delta_k} = \left( 1 - \left( \frac{\bar{P}_k}{P_k^*} \right)^{1/2} \right)^{5/2} \quad (1)$$

where  $\bar{g}_k$  is the amplitude of the sinusoidal-shaped asperity and  $P_k^*$  is the complete contact pressure at frequency level. In the current model, the same volume-loss approach employed by Green et al. [17] is used to calculate the gap at each radial position.

## 2.2 Mixed Lubrication Model

A mixed lubrication model is used to determine the hydrodynamic pressure distribution within the liquid flow. An average Reynolds equation [19] for incompressible fluid in polar coordinates is used which is given by

$$\frac{\partial}{\partial r} \left( \varphi r h^3 \frac{\partial p_{hyd}}{\partial r} \right) + \frac{1}{r} \frac{\partial}{\partial \theta} \left( \varphi h^3 \frac{\partial p_{hyd}}{\partial \theta} \right) = 12\eta r \frac{\partial h}{\partial t} \quad (2)$$

where  $r, \theta$  are the radial and azimuthal directions, respectively,  $p_{hyd}$  is the hydrodynamic pressure,  $h$  is the film thickness or the local gap,  $\varphi = 1 - 0.9e^{-0.56(h/\sigma)}$  is the pressure flow factor, and  $\eta$  is the dynamic viscosity of the working fluid. The second term in Eq. (2) disappears due to axisymmetric flow assumption. Also, it is assumed that the squeeze film effects is negligible (right-hand side of Eq. 2). Equation (2) along with the boundary conditions are solved numerically using Gauss-Seidel method to obtain the hydrodynamic pressure distribution.

## 3. Numerical Algorithm

A numerical algorithm is designed to solve the liquid flow problem. After introducing the input parameters (see Table 1), an initial value is selected for the radius of liquid flow,  $b_0$ . Next, the Reynolds equation is solved for the hydrodynamic pressure distribution. The sum of hydrodynamic pressure and pressure distribution due to external loading are inserted into the JS multiscale model to solve for the gap at each radial position. Then, a convergence test on tensile force is performed. In the lack of convergence, the updated values for radial gap is used in Reynolds equation to recalculate the hydrodynamic pressure distribution. When the convergence is acquired, the new value of  $b$  is calculated based on the relation between the pressure gradient and the rate of

change of liquid flow radius  $\left( \frac{\partial b}{\partial t} = -\frac{h_b^2}{12\eta} \frac{\partial p_{hyd}}{\partial r} \Big|_{r=b} \right)$ .

TABLE 1: Reference properties

Name	Symbol	Value
Nominal domain radius	$r_o$	3 cm
Radius of entrance hole	$r_i$	1 mm
Edge radius	$r'$	0.1 mm
Effective elastic modulus	$E'$	50 GPa
Liquid surface tension	$\gamma$	72.7 mN/m
Liquid viscosity	$\eta$	0.89 mPa.s
r.m.s. surface roughness	$\sigma$	0.4 $\mu\text{m}$

4. Results

A set of results of the numerical algorithm for the reference properties given in Table 1 in the presence of external load ( $P_{ext} = 30\text{N}$ ) is presented in this section. The results for the tensile force,  $F_t$ , and flow rate,  $Q$ , as the liquid spreads between the two surfaces as a function of time is shown in Figs. 4 and 5. The liquid flow starts at radius  $b = b_0$  and flows until the radius reaches the outer radius of the domain  $b = r_o$ . As it can be seen, the tensile force increases with time while the flow rate decreases with time. The results for the maximum tensile force,  $F_{t,max}$  and the initial flow rate,  $Q_{b_0}$ , versus the external load are shown in Fig. 6. As it can be seen, the maximum tensile force increases with the external load while the flow rate decreases with the external load.

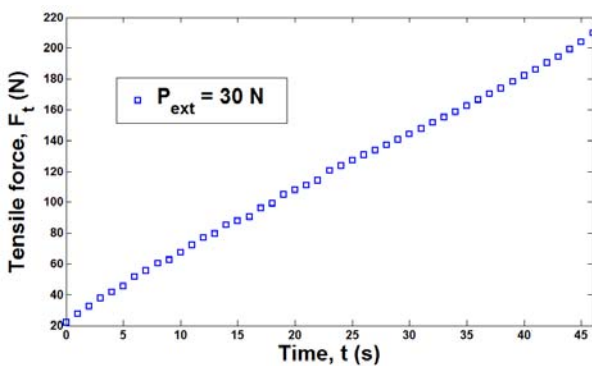


Fig.4. The results for the tensile force versus time.

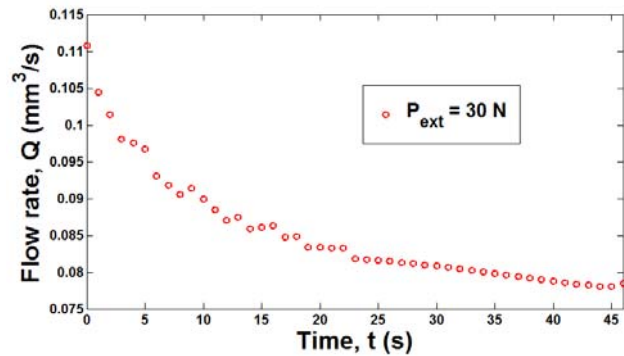


Fig.5. The results for the flow rate versus time.

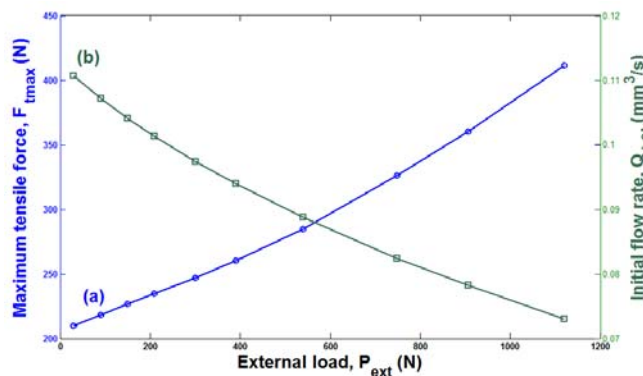


Fig.6. The results for (a) maximum tensile force, and (b) initial flow rate versus the external load.

## Conclusions

In this work, a numerical model for the liquid flow between two contacting rough surfaces due to capillary effects is presented. A contact model comprised of micro and macro level sub-models along with a mixed lubrication model are used to obtain the results. The results for the tensile force and flow rate are presented based on solving an iterative numerical algorithm. The results show that as the liquid spread between the two surfaces, the tensile force increases and flow rate decreases. The maximum tensile force increases as the external load is increased while the flow rate decreases with increasing external load.

## References

- [1] Tyree, M.T., 2003, “Plant hydraulics: the ascent of water,” *Nature*, 423(6943), pp. 923-923.
- [2] Fredlund, D.G., Rahardjo, H., 1993, “Soil mechanics for unsaturated soils,” *John Wiley & Sons*.
- [3] Maboudian, R., Howe, R.T., 1997, “Critical review: adhesion in surface micromechanical structures”, *Journal of Vacuum Science & Technology B*, 15(1), pp. 1-20.
- [4] Komvopoulos, K., 2003, “Adhesion and friction forces in microelectromechanical systems: mechanisms, measurement, surface modification techniques, and adhesion theory”, *Journal of adhesion science and technology*, 17(4), pp. 477-517.
- [5] Zhu, L., Xu, J., Zhang, Z., Hess, D.W., Wong, C., 2005, “Lotus effect surface for prevention of microelectromechanical system (MEMS) stiction,” *Electronic Components and Technology Conference, 2005 Proceedings 55th: IEEE*, pp. 1798-1801.
- [6] Hariri, A., Zu, J., Ben Mrad, R., 2007, “Modeling of wet stiction in microelectromechanical systems (MEMS),” *Microelectromechanical Systems, Journal of*, 16(5), pp. 1276-1285.
- [7] Tas, N.R., Mela, P., Kramer, T., Berenschot, J., van den Berg, A., 2003 “Capillarity induced negative pressure of water plugs in nanochannels,” *Nano Letters*, 3(1), pp. 1537-1540.
- [8] Deleanu, L., 2011, “A simplified model for partial journal and water lubrication”, *Hidraulica*, 1-2, pp. 71-77.
- [9] Streater, J.L., Jackson, R.L., 2009, “A model for the liquid-mediated collapse of 2-D rough surfaces”, *Wear*, 267(9), pp. 1436-1445.
- [10] Streater, J.L., 2009, “A model of liquid-mediated adhesion with a 2D rough surface,” *Tribology International*, 42(10), pp. 1439-1447.
- [11] Rostami, A., Streater, J.L., 2014, “A Model for Capillary Flow between Rough Surfaces,” *STLE Annual Meeting*.
- [12] Rostami, A., Streater, J.L., 2015, “Study of liquid-mediated adhesion between 3D rough surfaces: A spectral approach,” *Tribology International*, 84, pp. 36-47.
- [13] Rostami, A., Streater, J.L., 2015, “A Deterministic Approach to Studying Liquid-Mediated Adhesion Between Rough Surfaces,” *Tribology Letters*, 58(1), pp. 1-13.
- [14] Adamson, A.W., Gast, A.P., 1967, “Physical Chemistry of Surfaces”, *John Wiley & Sons*, New York.
- [15] Johnson, K., 1985, “Contact mechanics,” *Cambridge University Press*.
- [16] Garcia, N., Stoll, E., 1984, “Monte Carlo calculation for electromagnetic-wave scattering from random rough surfaces,” *Physical review letters*, 52(20), pp. 1798-1801.
- [17] Green, C.K., Streater, J.L., Haynes, C., Lara-Curzio, E., 2013, “A Computational Leakage Model for Solid Oxide Fuel Cell Compressive Seals,” *Journal of fuel cell science and technology*, 8(4), pp. 041003(1)-041003(9).
- [18] Rostami, A., Jackson, R.L., 2013, “Predictions of the average surface separation and stiffness between contacting elastic and elastic-plastic sinusoidal surfaces,” *Proceedings of the Institution of Mechanical Engineers, Part J: Journal of Engineering Tribology*, 227(12), pp. 1376-1385.
- [19] Hamrock, B.J., Schmid, S.R., Jacobson, B.O., 2004, “Fundamentals of fluid film lubrication,” *CRC press*.